THE JOURNAL OF PHYSICAL CHEMISTRY Letters

Letter

Cite This: J. Phys. Chem. Lett. 2018, 9, 6077−6081

pubs.acs.org/JPCL

Coherences of Bacteriochlorophyll a Uncovered Using 3D-Electronic Spectroscopy

Shawn Irgen-Gioro, Austin P. Spencer, William O. Hutson, and Elad Harel*

Department of Chemistry, Northwestern University, 2145 Sheridan Road, Evanston, Illinois 60208, United States

Supporting Information

ABSTRACT: Mapping the multidimensional energy landscape of photosynthetic systems is crucial for understanding their high efficiencies. Multidimensional coherent spectroscopy is well suited to this task but has difficulty distinguishing between vibrational and electronic degrees of freedom. In pigment−protein complexes, energy differences between vibrations within a single electronic manifold are similar to differences between electronic states, leading to ambiguous assignments of spectral features and diverging physical interpretations. An important control experiment is that of the pigment monomer, but previous attempts using multidimensional coherent spectroscopy lacked the sensitivity to capture the relevant spectroscopic signatures. Here we apply a variety of methods to rapidly acquire 3D electronic−vibrational spectra in seconds, leading to a mapping of the vibrational states of Bacteriochlorophyll *a* (BChl*a*) in solution. Using this information, we can distinguish features of proteins containing BChl*a* from the monomer subunit and show that many of the previously reported contentious spectral signatures are vibrations of individual pigments.

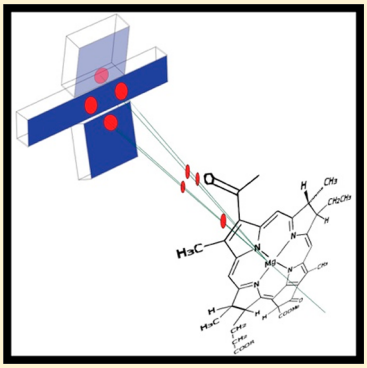

The evolution of photosynthetic bacteria paralleled the development of the early Earth and forms the energetic basis of life. Whereas the earliest photosystems were composed mainly of reaction centers, pigment−protein complexes (PPCs) that both absorbed light and executed reactions, millions of years of evolutionary optimization led to the development of entire PPC arrays capable of producing chemical energy at near-unit quantum efficiency.[1−3] Anaerobic photosynthetic bacteria, whose primary chromophore is Bacteriochlorophyll (BChl), has become a well-studied model system due to a relatively simple structure while retaining desirable photophysical properties. Located on the intracytoplasmic membrane of these bacteria, PPCs consist of pigments (BChl) noncovalently bound to structural units (apoproteins). The relative orientation of the BChl within the protein scaffolding modulates the energy states and coupling, in turn, dictating function.

Whereas the crystal structure of many of these PPCs has been resolved, the question of how structure affects energy-transfer dynamics remains open. Steady-state resonance Raman spectroscopies suggest that certain residues are coordinated to parts of the BChl macrocycle, but they fail to probe the femto/picosecond time-scale transfer process and time-dependent coupling between excitonic states.[4] Femtosecond time-resolved spectroscopy gives information on dynamics and also has the capability of detecting oscillatory features, or coherences, which arise from two energy states maintaining a quantum-mechanical phase relationship with each other. Using compressed laser pulses broad enough to span multiple states, the energy difference of the states that compose the superposition can be observed. Early experiments performed using pump−probe methods with short pulses on PPCs found coherences at the energy difference between excited electronic states.[5] The development of 2D electronic spectroscopy (2DES) allowed researchers to decongest complicated spectra over excitation and emission axes, resulting in an increased sensitivity for detecting coherences. This led to a flurry of studies on a variety of PPCs that reported coherences at the energy level difference between donor and acceptor states, suggesting the importance of these coherences in the energy-transfer process.[6−12] 2DES allows for simultaneously high spectral and temporal resolution, but it does not provide unambiguous assignment to the origin of the observed coherences to vibrational or electronic states. Typically, such discrimination is possible because electronic and vibrational motions exist on very different time scales and energies. However, in these PPCs, the energy level difference between excited electronic states is in the same energy regime as vibrations within a single electronic manifold. While this characteristic may lead to coupled vibrational-electronic (vibronic) states that mediate efficient transfer, it also leads to difficulties in understanding the nature of these states. Uncovering whether the coherences exist between vibrations on the same excitonic manifold or two different manifolds drastically changes the physical interpretation, but definitive assignment of the states involved has remained elusive.[13]

A key control experiment to understanding 2DES of coupled BChl systems is that of the BChl monomer, in which the vibrational and electronic coherences can be distinguished. This is achieved in our experiment because only one electronic state is within the bandwidth of the laser pulse, leading all coherences to

Received: July 16, 2018
Accepted: October 1, 2018
Published: October 1, 2018

DOI: 10.1021/acs.jpclett.8b02217
J. Phys. Chem. Lett. 2018, 9, 6077−6081

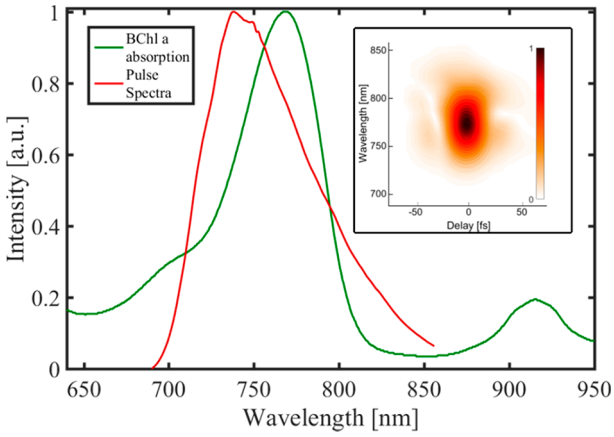

Figure 1. Near-IR absorption spectrum of BChl*a* compared with pulse spectrum, tuned for coverage of the Qy (S1) band. (Insert) TG-FROG trace of pulse used.

be vibrational in nature. Figure 1 shows the absorption spectrum of BChl*a* as well as the pulse spectrum used in our experiment. Some variants of nonlinear spectroscopy have reported Raman active modes of BChl*a*, but previous attempts at this control experiment have yielded no positive results; that is, no coherences were observed that coincided with those in the multichromophoric system.[14,15] Because resonance Raman experiments show a litany of low-frequency vibrations in BChl*a* and 2DES of PPCs shows strong coherences, the null results from BChl*a* have been used to justify nonvibrational origins of PPC coherences.[14,16] We find that the main reason for the discrepancies between 2DES experiments on BChl and on PPCs composed of them is the combination of multiple field−matter interactions that nonlinearly scale the transition moments, combined with poor dynamic range in the acquisition of weak signals. To address this issue, we overcome the typical $1/f$ noise (i.e., pink noise) distribution of most laboratory setting by acquiring the entire 128 × 916 × 2560, 32-bit data set in <2 s.[17] This setup is sensitive enough to capture the nonresonant response of the solvent, which is used to characterize the instrument. Using the solvent scan, the phase of our resonant scan can be recovered, and any frequencies of the solvent/instrument can be removed using a global analysis procedure, similar to one previoulsy described by Collini et al.[18] Shown diagrammatically in Figure 2 (top), the goal is to transform the original data, **Y**, into a matrix multiplication of two matrixes, **G** and **T**. Briefly, a m by N_2 basis set, **T**, is created, where m represents the number of bases and N_2 is the number of time points in the population time (the second time delay). The amplitudes of each of the basis sets, **G**, can be retrieved by taking the inverse of **T** and multiplying it by **Y**, or $\mathbf{G} = \mathbf{YT}^{-1}$. Using nonlinear regression to minimize $f(\mathbf{T}) = (\mathbf{Y} - \mathbf{GT})$ returns the basis set that best describes the data. This procedure decomposes the spectrum, as a particular basis (a $1 \times N_2$ vector) multiplied by its corresponding amplitude will create a 3D spectrum with only that component. Figure 2 (bottom) shows a few examples of bases (right) and their respective amplitudes (left). The beating frequencies that were found in the nonresonant scan were added to the basis set and fixed (not regressed). An example of a noise peak can be seen at the bottom of Figure 2, with characteristic features such as a negative decay time constant as well as having an amplitude that matches the intensity of the integrated 2DES along T. All of the bases that were found in the nonresonant scan are multiplied by their

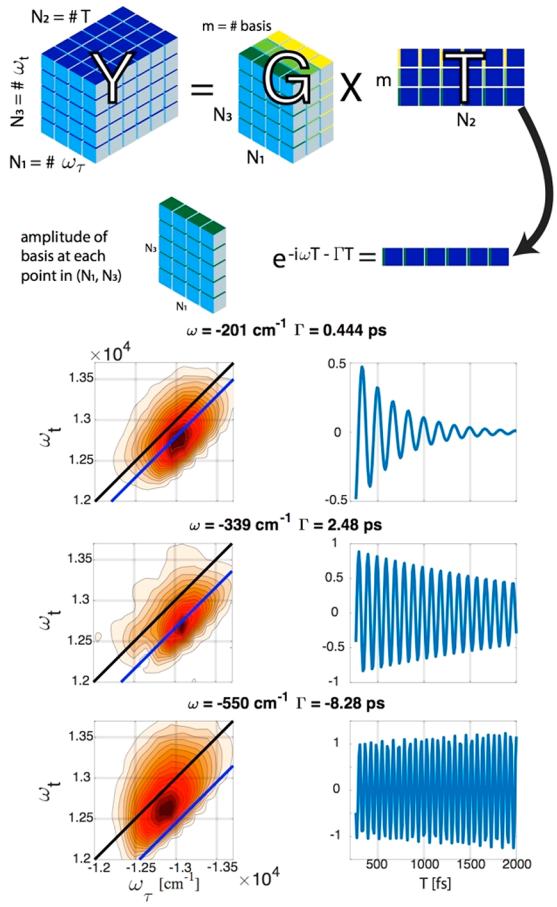

Figure 2. Using global analysis to identify noise peaks. (Top) The 3D data set can be thought of as a result of matrix multiplication between an $N_1{*}N_3 \times m$ matrix and an $m \times N_2$ matrix, where m is the number of bases. Each basis is a complex exponential, and the corresponding $N_1 \times N_3$ matrix represents the amplitude of that basis for every point in the 2D pump−probe spectrum. (Below) A few examples of the amplitudes and bases extracted from our BChl*a* spectra. Noise peaks are identified by the solvent-only scan and also do not decay within the T range (0−10 ps). The mode at 550 cm^{-1} is an example of a noise peak. Another trait that confirms this is a noise peak is that the max amplitude of the beat does not lie on the blue line, which is separated from the main diagonal by the oscillation energy. All frequencies that were found in the solvent-only scan are removed by multiplying their respective basis by their amplitude to create a noise-only spectrum, which is then subtracted from the original data.

corresponding amplitude to create a noise-only spectrum. This is then subtracted from our data to remove the contributions to the signal from those components. A detailed description of our experimental methods can be found in the Supporting Information (SI).

The real rephasing portion of the spectra is displayed in Figure 3 at T = 43 fs. The positive signal that lies on diagonal is a combination of excited-state emission (ESE) and ground-state bleach (GSB). An example point is chosen to view the time transient with the exponential decay terms removed and a Fourier transform performed to view the coherence frequencies. The coherences from every point in the 2D spectrum are then summed and are displayed in Figure 4 with previously reported transient grating (TG) frequencies by Scherer et al. shown as white lines.[19] It is worthwhile to note that projecting the 3D spectrum into 1D averages over weaker features, as seen in a

DOI: 10.1021/acs.jpclett.8b02217
J. Phys. Chem. Lett. 2018, 9, 6077−6081

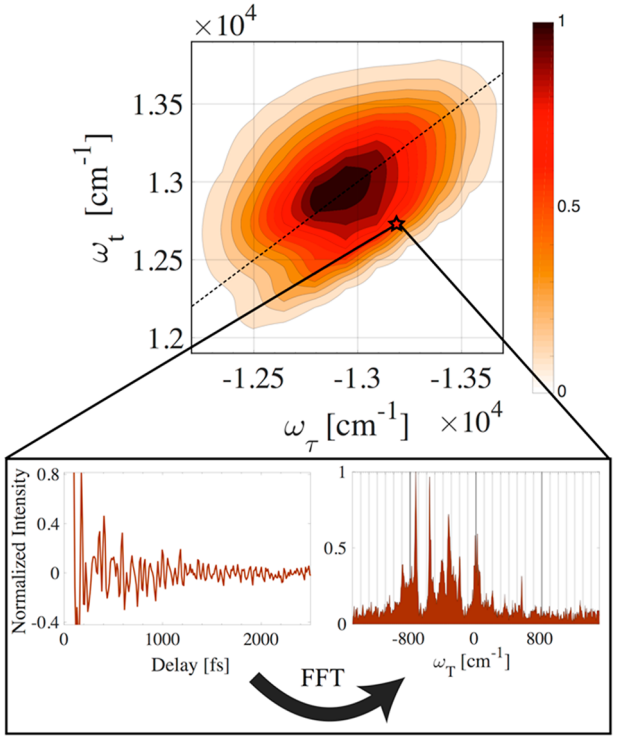

Figure 3. (Top) Real rephasing spectrum at $T = 43$ fs. An example point is picked from the structureless ground-state bleach feature at $\omega_\tau = -13\,389$ cm^{-1} and $\omega_t = 12\,776$ cm^{-1}, for which we display the time domain coherences along with the Fourier transform to extract the coherence frequency.

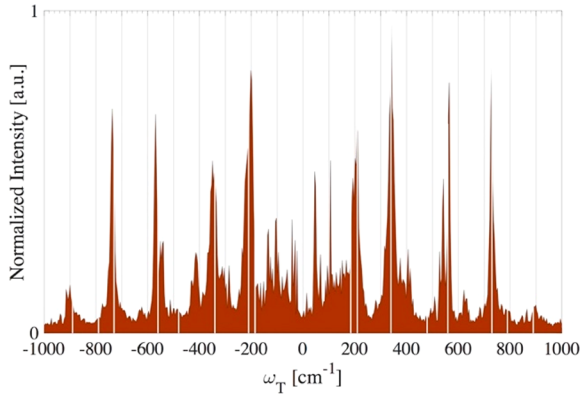

Figure 4. Summed coherence energies from all points in 2DES spectra. White lines represent reported frequencies from transient grating experiments.[19]

comparison of the beating spectrum in Figures 3 and 4. Our phased spectrum has the added benefit of distinguishing positive and negative frequencies, which informs us whether the coherences are on the ground or excited state. Because of the choice of phase-matching conditions ($\mathbf{k}_s = -\mathbf{k}_1 + \mathbf{k}_2 + \mathbf{k}_3$), the two rephasing pathways, ESE and GSB, differ in what happens in the second light−matter interaction.[20] The two pathways have been diagrammatically represented in the SI. ESE allows for both positive and negative frequencies, whereas GSB only allows for negative frequencies unless the system is initially in an excited vibrational state, which has significant population only for energies under $\sim kT = 207$ cm^{-1} in our room-temperature experiment. Whereas the GSB and ESE features are probably overlapping, meaning coherences probably also exist on the ground state, we can assign coherences to the excited state because of the roughly equal intensity positive and negative coherences.

Table 1. Comparing PPC and BChl*a* Coherence Frequencies

pigment−protein complex	reported coherence (cm^{-1})	BChl*a* coherence (cm^{-1})
Fenna−Matthews−Olson complex[7,21]	160, 200	201
Light-Harvesting Complex 2[12]	750	737
B820 subunit of Light-Harvesting Complex 1[11]	345, 416, 546, and 735	349, 413, 539, and 737

Comparing BChl*a* coherences to coherences observed in PPCs that contain BChl*a*, we find many similarities. A few examples are in Table 1. It can be seen that many previously reported coherences in PPCs are Franck−Condon active modes of the pigment monomer, making the long lifetimes of coherences less remarkable than if spatially separated electronic states could maintain correlation. Indeed, a recent study showed that Fenna−Matthews−Olson (FMO) coherence frequencies and lifetimes are insensitive to the electronic energies.[21] With definitive assignment of the origin of coherences, the identified vibrational states provide a basis for more in-depth interpretation of PPC 2DES. It can be seen that transitions in PPCs are not coupled to all of the BChl*a* vibrations available. Arranging the pigments in different geometric orientations, the PPC can select for useful vibrations given the purpose of the specific transition. For example, it has been shown experimentally that vibrational−exciton resonance enhances energy-transfer rates.[22] Even within this framework, it has been unclear up until now whether useful vibrations in PPCs originate from collective motions or from individual pigments. In LH2, the mode that is implicated in mode-assisted transport is at 735 cm^{-1}. Using this study to assign the origin of the coherence and previous work in normal-mode analysis of Raman studies, we can assign the mode that participates in the B800−B850 transfer step to symmetric in-plane bend of $NC_aC_m(\alpha)$.[23] Whereas most of the coherences can be attributed to pigment vibrations, some are still uncertain. In particular, FMO has two low-frequency modes around 160 and 200 cm^{-1}, only one of which definitively corresponds to coherences found in BChl*a*.[21] The 200 cm^{-1} mode has been reported as Mg-sensitive and has been assigned to be an out-of-plane MgN deformation.[23,24] The 160 cm^{-1} mode, which is also a strong coherence in LH2 and B820, is not observed with high intensity in our experiment or in previous TG experiments.[15,19] However, previous shifted excitation Raman difference spectra show a 177 cm^{-1} mode with larger intensity than both the 212 cm^{-1} mode and the 730 cm^{-1} mode.[16] The mode has also been characterized in the excited state using nonphotochemical hole burning and is observed at 166 cm^{-1}.[25] The low relative intensity in this particular experiment is puzzling, especially knowing the mode's strength in PPC 2DES and monomer Raman experiments.

Although not all coherences can be attributed to pigment vibrations, most of the previously reported coherences at the electronic energy level differences can be. Much attention has been placed on the electronic states of PPCs, but the vibrational landscape is equally important. Strongly coupled vibrations can broaden electronic transitions, allowing for better spectral overlap, as well as funnel energy to the vibrational ground state through internal relaxation. While the exact role of vibrations in PPCs is still up for debate, the ability to assign spectral signatures

DOI: 10.1021/acs.jpclett.8b02217
J. Phys. Chem. Lett. 2018, 9, 6077−6081

of coherences in PPCs to vibrations of the monomer subunit is an important step.

Whereas this study can assign many of the long-lived coherences to vibrations, coherences that decay with a lifetime of ∼100 fs are not found in the BChl spectra. In fact, if coherence frequencies and lifetimes are fit for $T > 250$ fs and projected back to $T = 0$, then only population dynamics remain. Contrastingly, in LH2, mutant studies with the B800 band removed found a fast dephasing coherence assigned to the B850 and B850*, and simulations back up the idea of a rapidly dephasing B800 and B850 excitonic coherence on that time scale.[26,27] In FMO, similar <100 fs dephasing is seen, also assigned to excitonic coherences.[28] Thus, with definitive assignment of long-lived coherences as vibrations and lack of fast dephasing coherences in the monomer, these previously reported ∼100 fs dephasing coherences are most likely excitonic in nature, matching expected dephasing rates. Using the same global analysis technique used to remove the solvent response from our data, long-lived coherences can be removed to better reveal the excitonic lifetimes and frequencies. Knowing the long-lived coherences are vibrations and rapidly dephasing coherences are excitonic helps align the interpretation of 2DES with physical models.

Improvements in 2DES experimental data collection and analysis have enabled us to extract the vibrational coherence energies of BChl*a*. This has demonstrated that many of the previously reported coherences that were attributed to long-lived coherences between excited electronic states are most likely vibrations in individual pigments. However, 2DES of BChl does not display fast dephasing lifetimes, demonstrating that previously reported coherences that dephase at ∼100 fs lifetime are most likely excitonic in nature. It is still unknown why the vibrational coherence energies match up with many of the excitonic energy gaps reported in ultrafast energy transfer in PPCs. With the ability to provide vibrations at a variety of energies and easily tune the electronic structure through spatial manipulation, it can be seen why BChl*a* is used as a pigment in a variety of PPCs. Whether PPCs developed their electronic states to have energy gaps the same as the vibrations available from the BChl, the PPCs and BChl structures coevolved with each other, or the energies matching up is coincidental remains an open question.

■ ASSOCIATED CONTENT

Supporting Information

The Supporting Information is available free of charge on the ACS Publications website at DOI: 10.1021/acs.jpclett.8b02217.

Experimental methods, global analysis, and ESE versus GSB pathways (PDF)

Raw data file of 1D coherences (Figure 4 in main manuscript) (TXT)

■ AUTHOR INFORMATION

Corresponding Author

*E-mail: elharel@northwestern.edu.

ORCID

Austin P. Spencer: 0000-0003-4043-2062

Elad Harel: 0000-0003-3007-0993

Author Contributions

S.I.-G. grew the cells, isolated the sample, and performed experiments. S.I.-G. and E.H. analyzed the data and wrote the paper. A.P.S., W.O.H., and S.I.-G. built the setup.

Notes

The authors declare no competing financial interest.

■ ACKNOWLEDGMENTS

We thank the recombinant protein production core, specifically Dr. Sergii Pshenychnyi, at Northwestern University for their help, advice, and equipment lending. Also, we thank Prof. Pamela Parkes-Loach and Prof. Paul Loach in their guidance in growing bacteria. This work was supported by the Air Force Office of Scientific Research (FA9550-14-1-0005), and the Packard Foundation (2013-39272) in part.

■ REFERENCES

(1) Olson, J. M.; Pierson, B. K. Evolution of Reaction Centers in Photosynthetic Prokaryotes. *Int. Rev. Cytol.* **1987**, *108*, 209−248.

(2) Sener, M.; Strumpfer, J.; Singharoy, A.; Hunter, C. N.; Schulten, K. Overall Energy Conversion Efficiency of a Photosynthetic Vesicle. *eLife* **2016**, *5*, No. e09541.

(3) Scheer, H. *Chlorophylls*; CRC-Press: 1991.

(4) Robert, B.; Lutz, M. Structures of Antenna Complexes of Several Rhodospirillales from Their Resonance Raman Spectra. *Biochim. Biophys. Acta, Bioenerg.* **1985**, *807*, 10−23.

(5) Savikhin, S.; Buck, D. R.; Struve, W. S. Oscillating Anisotropies in a Bacteriochlorophyll Protein: Evidence for Quantum Beating between Exciton Levels. *Chem. Phys.* **1997**, *223*, 303−312.

(6) Engel, G. S.; Calhoun, T. R.; Read, E. L.; Ahn, T.-K.; Mančal, T.; Cheng, Y.-C.; Blankenship, R. E.; Fleming, G. R. Evidence for Wavelike Energy Transfer through Quantum Coherence in Photosynthetic Systems. *Nature* **2007**, *446*, 782.

(7) Panitchayangkoon, G.; Hayes, D.; Fransted, K. A.; Caram, J. R.; Harel, E.; Wen, J.; Blankenship, R. E.; Engel, G. S. Long-Lived Quantum Coherence in Photosynthetic Complexes at Physiological Temperature. *Proc. Natl. Acad. Sci. U. S. A.* **2010**, *107*, 12766.

(8) Collini, E.; Wong, C. Y.; Wilk, K. E.; Curmi, P. M. G.; Brumer, P.; Scholes, G. D. Coherently Wired Light-Harvesting in Photosynthetic Marine Algae at Ambient Temperature. *Nature* **2010**, *463*, 644.

(9) Romero, E.; Augulis, R.; Novoderezhkin, V. I.; Ferretti, M.; Thieme, J.; Zigmantas, D.; van Grondelle, R. Quantum Coherence in Photosynthesis for Efficient Solar-Energy Conversion. *Nat. Phys.* **2014**, *10*, 676.

(10) Calhoun, T. R.; Ginsberg, N. S.; Schlau-Cohen, G. S.; Cheng, Y.-C.; Ballottari, M.; Bassi, R.; Fleming, G. R. Quantum Coherence Enabled Determination of the Energy Landscape in Light-Harvesting Complex Ii. *J. Phys. Chem. B* **2009**, *113*, 16291−16295.

(11) Ferretti, M.; Novoderezhkin, V. I.; Romero, E.; Augulis, R.; Pandit, A.; Zigmantas, D.; Grondelle, R. v. The Nature of Coherences in the B820 Bacteriochlorophyll Dimer Revealed by Two-Dimensional Electronic Spectroscopy. *Phys. Chem. Chem. Phys.* **2014**, *16*, 9930−9939.

(12) Harel, E.; Engel, G. S. Quantum Coherence Spectroscopy Reveals Complex Dynamics in Bacterial Light-Harvesting Complex 2 (Lh2). *Proc. Natl. Acad. Sci. U. S. A.* **2012**, *109*, 706.

(13) Fassioli, F.; Dinshaw, R.; Arpin, P. C.; Scholes, G. D. Photosynthetic Light Harvesting: Excitons and Coherence. *J. R. Soc., Interface* **2014**, *11*, 20130901.

(14) Fransted, K. A.; Caram, J. R.; Hayes, D.; Engel, G. S. Two-Dimensional Electronic Spectroscopy of Bacteriochlorophyll a in Solution: Elucidating the Coherence Dynamics of the Fenna-Matthews-Olson Complex Using Its Chromophore as a Control. *J. Chem. Phys.* **2012**, *137*, 125101.

(15) Yue, S.; Wang, Z.; Leng, X.; Zhu, R.-D.; Chen, H.-L.; Weng, Y.-X. Coupling of Multi-Vibrational Modes in Bacteriochlorophyll a in Solution Observed with 2d Electronic Spectroscopy. *Chem. Phys. Lett.* **2017**, *683*, 591−597.

(16) Cherepy, N. J.; Shreve, A. P.; Moore, L. J.; Franzen, S.; Boxer, S. G.; Mathies, R. A. Near-Infrared Resonance Raman Spectroscopy of the Special Pair and the Accessory Bacteriochlorophylls in Photosynthetic Reaction Centers. *J. Phys. Chem.* **1994**, *98*, 6023−6029.

DOI: 10.1021/acs.jpclett.8b02217
J. Phys. Chem. Lett. 2018, 9, 6077−6081

(17) Feng, Y.; Vinogradov, I.; Ge, N.-H. General Noise Suppression Scheme with Reference Detection in Heterodyne Nonlinear Spectroscopy. *Opt. Express* **2017**, *25*, 26262−26279.
(18) Volpato, A.; Bolzonello, L.; Meneghin, E.; Collini, E. Global Analysis of Coherence and Population Dynamics in 2d Electronic Spectroscopy. *Opt. Express* **2016**, *24*, 24773−24785.
(19) Amett, D. C.; Yang, T. S.; Scherer, N. F. Optical and Vibrational Coherence in Bacteriochlorophyll A. *Time-Resolved Vib. Spectrosc., Proc. Int. Conf. TRVS* **1997**, 131−135.
(20) Mukamel, S. *Principles of Nonlinear Optical Spectroscopy*; Oxford University Press: 1995.
(21) Maiuri, M.; Ostroumov, E. E.; Saer, R. G.; Blankenship, R. E.; Scholes, G. D. Coherent Wavepackets in the Fenna−Matthews−Olson Complex Are Robust to Excitonic-Structure Perturbations Caused by Mutagenesis. *Nat. Chem.* **2018**, *10*, 177.
(22) Womick, J. M.; Moran, A. M. Vibronic Enhancement of Exciton Sizes and Energy Transport in Photosynthetic Complexes. *J. Phys. Chem. B* **2011**, *115*, 1347−1356.
(23) Ceccarelli, M.; Lutz, M.; Marchi, M. A Density Functional Normal Mode Calculation of a Bacteriochlorophyll a Derivative. *J. Am. Chem. Soc.* **2000**, *122*, 3532−3533.
(24) Czarnecki, K.; Diers, J. R.; Chynwat, V.; Erickson, J. P.; Frank, H. A.; Bocian, D. F. Characterization of the Strongly Coupled, Low-Frequency Vibrational Modes of the Special Pair of Photosynthetic Reaction Centers Via Isotopic Labeling of the Cofactors. *J. Am. Chem. Soc.* **1997**, *119*, 415−426.
(25) van der Laan, H.; Smorenburg, H. E.; Schmidt, T.; Völker, S. Permanent Hole Burning with a Diode Laser: Excited-State Dynamics of Bacteriochlorophyll in Glasses and Micelles. *J. Opt. Soc. Am. B* **1992**, *9*, 931−940.
(26) Singh, V. P.; Westberg, M.; Wang, C.; Dahlberg, P. D.; Gellen, T.; Gardiner, A. T.; Cogdell, R. J.; Engel, G. S. Towards Quantification of Vibronic Coupling in Photosynthetic Antenna Complexes. *J. Chem. Phys.* **2015**, *142*, 212446.
(27) Caycedo-Soler, F.; Lim, J.; Oviedo-Casado, S.; van Hulst, N. F.; Huelga, S. F.; Plenio, M. B. Theory of Excitonic Delocalization for Robust Vibronic Dynamics in Lh2. *J. Phys. Chem. Lett.* **2018**, *9*, 3446−3453.
(28) Thyrhaug, E.; Tempelaar, R.; Alcocer, M. J. P.; Žídek, K.; Bína, D.; Knoester, J.; Jansen, T. L. C.; Zigmantas, D. Identification and Characterization of Diverse Coherences in the Fenna−Matthews−Olson Complex. *Nat. Chem.* **2018**, *10*, 780−786.

DOI: 10.1021/acs.jpclett.8b02217
J. Phys. Chem. Lett. 2018, 9, 6077−6081